EUROPEAN ORGANIZATION FOR NUCLEAR RESEARCH

CERN/PPE 92-94
18 May 1992

FURTHER STUDY OF THE $E/f_1(1420)$ MESON IN CENTRAL PRODUCTION

WA76 Collaboration
Athens-Bari-Birmingham-CERN-Collège de France

T.A. Armstrong[4a], M. Benayoun[5], I.J. Bloodworth[3], J.N. Carney[3], C.J. Dodenhoff[3], C. Evangelista[2], B.R. French[4], B. Ghidini[2], M. Girone[2], A. Jacholkowski[4], J. Kahane[5], J.B. Kinson[3], A. Kirk[4], K. Knudson[4], V. Lenti[2], Ph. Leruste[5], A. Malamant[5], J.L. Narjoux[5], F. Navach[2], A. Palano[2], N. Redaelli[4b], L. Rossi[4c], M. Sené[5], R. Sené[5], M. Stassinaki[1], G. Vassiliadis[1], O. Villalobos Baillie[3], M.F. Votruba[3] and G. Zito[2]

Abstract

We have studied the reactions $(\pi^+/p)p \to (\pi^+/p)(K\bar{K}\pi)p$, where the $K\bar{K}\pi$ system is centrally produced, at 85 GeV/c and 300 GeV/c using the CERN Omega spectrometer. A spin-parity analysis of the $K^0_S K^{\pm}\pi^{\mp}$ system shows the presence of a strong $J^{PG} = 1^{++}$ signal which we identify as the $E/f_1(1420)$ meson. We also find evidence for the decay $E/f_1(1420) \to K^0_S K^0_S \pi^0$ which determines the C-parity of this state to be positive. Alternative explanations of the data have been tested and ruled out. Hence we obtain the quantum numbers of the $E/f_1(1420)$ to be $I^G(J^{PC}) = 0^+(1^{++})$.

Submitted to Zeitschrift für Physik C

1) Athens University, Nuclear Physics Department, Athens, Greece
2) Dipartimento di Fisica dell'Università and Sezione INFN, Bari, Italy
3) University of Birmingham, Physics Department, Birmingham, U.K.
4) CERN, European Organization for Nuclear Research, Geneva, Switzerland
5) Collège de France, Paris, France
a) Present address: Pennsylvania State University, University Park, USA
b) Present address: INFN and Dipartimento di Fisica, Milan, Italy
c) Present address: INFN and Dipartimento di Fisica, Genoa, Italy

1. INTRODUCTION

One of the most interesting resonances from the point of view of the possible existence of non-$q\bar{q}$ states is the $J^{PC} = 1^{++}$ $E/f_1(1420)$ meson. Its classification in the quark model is still unclear, its quantum numbers are sometimes subjected to criticisms and its interpretation as a normal hadronic resonance is not without problems. A further complication in the E mass region is that the number of states which contribute to the enhancement observed in the mass spectrum changes from one experiment to the other. The actual experimental situation in the 1.4 GeV mass region, which has led to the so called E/ι puzzle, is summarized below:

a) A resonance in the $K\bar{K}\pi$ system, called the E meson, was discovered in $p\bar{p}$ annihilation at rest [1] and in this process its quantum numbers were determined to be $J^{PC} = 0^{-+}$ [2,3].

b) A $K\bar{K}\pi$ state in the same mass region was observed in $\pi^- p$ interactions with contradicting results: one experiment found $J^{PC} = 1^{++}$ [4], while other experiments found $J^{PC} = 0^{-+}$ [5,6].

c) A strong $K\bar{K}\pi$ signal in the 1.4 GeV mass region has been observed in central hadron-hadron collisions and, assuming I=0, its quantum numbers have been found to be $J^{PC} = 1^{++}$ [7].

d) Several experiments have reported a signal in the E meson mass region in $\gamma\gamma^*$ collisions [8] having quantum numbers $J^{PC} = 1^{++}$ where the parity assignment is favoured but still requires confirmation.

e) Radiative J/ψ decay shows evidence for a strong signal (named ι) which recently has been found to be composed of a mixture of two resonances with $J^{PC} = 0^{-+}$ and one resonance with $J^{PC} = 1^{++}$ [9].

f) Hadronic J/ψ decay to $\omega K\bar{K}\pi$ also shows evidence for production of a $J^{PC} = 1^{++}$ resonance in the $K\bar{K}\pi$ system [10].

This confusing experimental situation has led, in the last ten years, to an intense phenomenological debate on the possibility that one or more of these states are non-$q\bar{q}$ mesons such as glueballs, hybrids or multiquark states [11].

The $J^{PC} = 1^{++}$ E meson, now called $f_1(1420)$, was considered, until recently, to be the $s\bar{s}$ member of the axial nonet. However, this hypothesis is in contradiction with several experimental results, namely:

i) It is not produced in K^- induced reactions, where an $s\bar{s}$ state should prominently appear. On the other hand a different axial resonance, the $f_1(1520)$, has been discovered in these reactions [12], which has the expected properties for being the $s\bar{s}$ member of the axial meson nonet.

ii) The pattern observed in hadronic J/ψ decay ($J/\psi \to \omega E$ seen, $J/\psi \to \phi E$ not seen) is inconsistent with a mainly $s\bar{s}$ composition of the $E/f_1(1420)$ meson [13]. The same conclusion comes from the observed rates for production of this resonance in $\gamma\gamma^*$

collisions: Γ_E is too large for a mainly strange meson [14].

These arguments lead to two possibilities: either the $E/f_1(1420)$ belongs to the axial nonet with a mixing angle far from the ideal one leaving the $f_1(1520)$ as an extra state or, more reasonably, the $E/f_1(1420)$ is the extra resonance which does not fit into the quark model. In the latter case it is interesting to understand what it really is: a hybrid meson [15], a $K^*\bar{K}$ molecule or a multiquark state [14,16].

In addition to these problems, it has also been suggested by some authors [17] who have performed an analysis on the Dalitz plot projections from published data from the Omega-WA76 experiment, that the C parity determination of the $E/f_1(1420)$ meson is indeed wrong and that we are in fact dealing with the $J^{PC} = 1^{+-}$ $h_1(1420)$ meson.

In order to answer this criticism and to contribute to the solution of the problems stated above we have reanalyzed the full data sample coming from all the runs of the Omega-WA76 experiment. This experiment has been performed in two different runs. In the first period data have been collected with incident π^+ and p beams at 85 GeV/c beam momentum. In the second run the beam momentum was increased to 300 GeV/c but only data with incident protons have been collected. Details on trigger conditions, data processing and event selection for the two experiments have been given in previous publications [7,18].

This paper is organized as follows. In section 2 we present the mass spectra and the results obtained in these experiments which are relevant for the understanding of the $E/f_1(1420)$ properties. In section 3 the results from the spin-parity analysis of the $K^0_S K^{\pm}\pi^{\mp}$ system are presented. Section 4 tests other possible explanations of the data and finally the results are summarized in section 5.

2. MASS SPECTRA

The reactions:

$$\pi^+ p \rightarrow \pi^+ (K^0_S K^{\pm}\pi^{\mp}) p \tag{1}$$

at 85 GeV/c and

$$pp \rightarrow p(K^0_S K^{\pm}\pi^{\mp}) p \tag{2}$$

at 85 and 300 GeV/c, have been selected from the sample of 4-prong events having one reconstructed K^0_S and which balance momentum. The K/π ambiguity in the mass assignment of the positive and negative particles was partly solved by using the Cherenkov information and partly by requiring the Ehrlich mass squared [19], computed on the two K's, and shown in fig. 1(a), to be in the range $0.20 \leq m^2_X \leq 0.56$ GeV^2.

The combined $K^0_S K^{\pm}\pi^{\mp}$ mass spectrum is shown in fig. 1(b) where prominent signals corresponding to $f_1(1285)$ and $E/f_1(1420)$ mesons can be seen.

We have also searched, in the same experiment, for the reactions

$$pp \rightarrow p(K^+K^-\pi^0) p \tag{3}$$

and

$$pp \rightarrow p(K^0_S K^0_S \pi^0)p \tag{4}$$

at 300 GeV/c incident proton momentum.

Reaction (3) has been selected from the sample of 4-prong events balancing momentum and having only 2γ reconstructed in the electromagnetic calorimeter. One of the two K's was required to be identified as K or ambiguous K/p by the Cherenkov information while the other K, if reaching the Cherenkov system, was required to have a mass assignment consistent with being a K. Fig. 2(a) shows the $\gamma\gamma$ effective mass distribution for these events where a clear π^0 peak can be seen. Selecting the 2γ mass in the π^0 peak we obtain the Ehrlich mass squared (computed for the two K's) shown in fig. 2(b) where the peak centered at the square of the K mass is the signal of reaction (3). The $K^+K^-\pi^0$ effective mass distribution is shown in fig. 2(c) and shows enhancements in the $f_1(1285)$ and $E/f_1(1420)$ regions. An inspection of the K^+K^- mass distribution (fig. 2(d)) shows little evidence for the production of the $\phi(1020)\pi^0$ final state where a possible exotic resonance has been reported [20].

Since resonances observed to decay to $K^0_S K^0_S \pi^0$ can only have positive C-parity we have searched for the $E/f_1(1420)$ meson in reaction (4) which has been selected from the sample of events balancing momentum and energy but belonging to two different topologies.

a) Fully reconstructed events having two measured K^0_S and only two γ's coming from a π^0 decay reconstructed in the electromagnetic calorimeter.

b) Events having two reconstructed K^0_S but only one gamma detected in the electromagnetic calorimeter. In this case the missing γ has been reconstructed as a missing particle constrainted to come from a π^0 decay.

The K^0_S signals for samples a) and b) are shown in fig. 3(b) and 3(d) respectively and the corresponding $K^0_S K^0_S \pi^0$ effective mass distributions for the two samples are shown in fig. 3(a) and 3(c) respectively. The sum of the two histograms is shown in fig. 3(e). Requiring any $K^0_S \pi^0$ mass combination to be in the K^{*0} region, we obtain the $K^*\bar{K}$ mass spectrum shown shaded in fig. 3(e). While the few events present in this channel are not useful for spin analysis, the enhancement (within the limited statistics) in the 1.4 GeV region of the $K^0_S K^0_S \pi^0$ mass spectrum is consistent with the presence of the E signal and supports the positive C-parity assignment for this state.

In order to search for other possible decay modes of the $E/f_1(1420)$, we have compared the $K^0_S K^\pm \pi^\mp$ mass spectrum (fig. 4(a)) with those from $2\pi^+2\pi^-$ [21], $\eta\pi^+\pi^-$ [22] and $\rho^0\gamma$ [23] (figs. 4(b,c,d) respectively). While we observe a clear $f_1(1285)$ signal in all the spectra, no enhancements are visible (except for the $2\pi^+2\pi^-$ channel) in the $E/f_1(1420)$ region. In the $2\pi^+2\pi^-$ channel we observe a structure with $m = 1449 \pm 4$ MeV and $\Gamma = 78 \pm 18$ MeV. This mass value is not consistent (a 4σ effect) with the value obtained from the study of the $K^0_S K^\pm \pi^\mp$ channel. This result is confirmed by a spin analysis and by the study of the production mechanism of the resonances observed in both the $K^0_S K^\pm \pi^\mp$ and $2\pi^+2\pi^-$ channels [21]. We conclude, therefore, that the only observed decay mode of the

$E/f_1(1420)$ meson is $K^*\bar{K}$ and we set upper limits of

$$B.R.(E/f_1(1420) \to \eta\pi\pi) < 0.1 \quad 95\%\ C.L.$$

and

$$B.R.(E/f_1(1420) \to \rho^0\gamma) < 0.08 \quad 95\%\ C.L.$$

3. SPIN-PARITY ANALYSIS OF THE $K^0_S K^\pm\pi^\mp$ SYSTEM.

A spin parity analysis of the low mass region of the $K^0_S K^\pm\pi^\mp$ system has been performed using the Zemach tensor formalism [24,4] through fits to the Dalitz plot distribution. $\delta/a_0(980)\pi$ and $K^*\bar{K}$ intermediate states with $J^{PG} = 0^{-+}, 1^{++}, 1^{-+}$ and 1^{+-} have been considered. In the fitting procedure, contributions consistent with zero in all the mass range have been removed from the fit.

The results of the maximum likelihood fits as functions of the $K^0_S K^\pm\pi^\mp$ mass are shown in fig. 5 and can be summarized as follows:

a) The $J^{PG} = 1^{++}$ $K^*\bar{K}$ wave dominates the spectrum and shows a clear signal at the $E/f_1(1420)$ mass. The fit shown in fig. 5 gives $m = 1430 \pm 4$ MeV and $\Gamma = 58 \pm 10$ MeV as $E/f_1(1420)$ parameters.

b) There is a small $J^{PG} = 0^{-+}$ $K^*\bar{K}$ contribution. A fit with a simple Breit-Wigner gives $m = 1425 \pm 13$ MeV and $\Gamma = 71 \pm 31$ MeV.

c) There is a relatively small 1^{+-} contribution.

The absence of any $\delta/a_0(980)\pi$ contribution in the 1.4 GeV mass region agrees well with the observed absence of a signal in the $\eta\pi^+\pi^-$ system in the same experiment [22].

We thus confirm production in the central region of the $E/f_1(1420)$ with a single decay mode $K^*\bar{K}$ and determine its quantum numbers J^{PG} to be 1^{++}. This result, combined with the positive C-parity assignment coming from the evidence of the decay $E/f_1(1420) \to K^0_S K^0_S \pi^0$, allows us, using the relation $G = C(-1)^I$ to determine the isospin to be zero. Therefore the quantum numbers of the $E/f_1(1420)$ are determined to be $I^G(J^{PC}) = 0^+(1^{++})$.

No evidence is found for $\eta(1400) \to \delta/a_0(980)\pi$ which has been reported in π induced reactions [5,6] and in J/ψ radiative decay [9].

4. TEST OF A POSSIBLE ALTERNATIVE DESCRIPTION OF THE DATA

It has been argued, in ref. [17], on the basis of a study of the Dalitz plot projections in the $E/f_1(1420)$ region and assuming I=0, that the C-parity of this state is negative.

This would mean, in fact, that we are observing the $h'(1420)$ meson with $J^{PC} = 1^{+-}$. The authors of ref. [17] claim that proper combinations of $J^{PC} = 0^{-+}$ and 1^{+-} waves can fit the data better than 1^{++}. We note that:

a) The comparisons are performed at a fixed mass of the $K\bar{K}\pi$ system and the Breit-Wigner shape of the resonance was not taken into account in their analysis;

b) Use of only the Dalitz plot projections does not take into account the two-dimensional correlation.

For these reasons the comparison between data and expectations can only be qualitative. It has also been suggested, in ref. [17], that good spin-parity indicators are the angles θ_1 and θ_2 shown in fig. 6. Here θ_1 is the angle formed between the $K^{\pm}$ and the $\pi^{\mp}$ in the $K^0K^{\pm}$ rest frame and θ_2 is the angle between the K^0 and the $\pi^{\mp}$ in the $\pi^{\mp}K^{\pm}$ rest frame. Monte-Carlo simulations of θ_1 and θ_2 for E decays via phase space (50%) and $J^{PC} = 0^{-+}, 1^{++}, 1^{+-}$ $K^*\bar{K}$ are shown in fig. 6.

In this section we show the results of a comparison between fits performed on the Dalitz plot using the full set of waves described in the previous section:

$$\text{hypothesis} \quad A : (J^{PC} = 0^{-+}, 1^{++}, 1^{+-}, \text{phase space})$$

and the solution claimed in ref. [17]:

$$\text{hypothesis} \quad B : (J^{PC} = 0^{-+}, 1^{+-}, \text{phase space})$$

Defining the $E/f_1(1420)$ to be in the region $1.37 < m(K\bar{K}\pi) < 1.49$ GeV (2048 events, see fig. 7 for the Dalitz plot) we have performed a fit using hypothesis A. We obtain, as fraction for each contribution:

$$0^{-+} = 0.11 \pm 0.03$$

$$1^{++} = 0.44 \pm 0.05$$

$$1^{+-} = 0.14 \pm 0.03$$

$$\text{phase space} = 0.31 \pm 0.04$$

and log(Likelihood)=565.

This solution has been compared with the data by performing a Monte-Carlo simulation where events have been generated according to the experimental mass distribution of the $K^0_S K^{\pm}\pi^{\mp}$ system in the $E/f_1(1420)$ region weighted by the solution found by the fit. The $E/f_1(1420)$ Dalitz plot projections and the θ_1 and θ_2 angular distributions are compared with the Monte-Carlo simulation in fig. 8. We observe that we obtain a good agreement between data and Monte-Carlo simulation in all the distributions. In order to have a quantitative measurement of the quality of the fit we have computed the χ^2 on the two-dimensional Dalitz plot distribution. We obtain $\chi^2/\text{NDF} = 218/210$ corresponding to a 34% probability. Here NDF is the number of bins in the Dalitz plot with non-zero events minus the number of parameters used in the maximum likelihood fit (three in this case).

Similarly, we have then tested hypothesis B. We obtain, in this case, a much worse likelihood (log(Likelihood)= 520) and fractions:

$$0^{-+} = 0.28 \pm 0.02$$

$$1^{+-} = 0.37 \pm 0.02$$

$$\text{phase space} = 0.35 \pm 0.04$$

We have then generated a Monte-Carlo simulation with this solution which is compared with the experimental data distributions in fig. 9. We note that, even if we can obtain some description of the data, the quality of the fit is worse with respect to the previous case. Computing the χ^2 on the Dalitz plot results in a χ^2/NDF=287/214 corresponding to a probability of 6×10^{-4}.

We conclude, from this analysis, that both hypotheses ($J^{PC} = 0^{-+}, 1^{++}, 1^{+-}$, phase space) and ($J^{PC} = 0^{-+}, 1^{+-}$, phase space) can qualitatively describe the data but the first hypothesis is strongly favoured (probability=34% against $6. \times 10^{-4}$) with respect to the second. It is also clear, from figs. 8 and 9, that the difference between hypotheses A and B is not striking and cannot easily be detected working only on the projections of the Dalitz plot and at a fixed mass. By performing two-dimensional fits we find that the best description of the data is given by a dominance of the 1^{++} wave with weak contributions of 0^{-+} and 1^{+-} waves.

5. CONCLUSIONS

In conclusion, we have studied the reactions $(\pi^+/p)p \to (\pi^+/p)(K\bar{K}\pi)p$, where the $K\bar{K}\pi$ system is centrally produced, at 85 GeV/c and 300 GeV/c, using the CERN Omega spectrometer. A spin-parity analysis of the $K^0_S K^{\pm}\pi^{\mp}$ system shows the presence of a strong $J^{PG} = 1^{++}$ signal which we identify as the $E/f_1(1420)$ meson. We also find evidence for the decay $E/f_1(1420) \to K^0_S K^0_S \pi^0$ which determines the C-parity of this state to be positive. Alternative explanations of the data have been tested and ruled out. Hence we obtain the quantum numbers of the $E/f_1(1420)$ to be $I^G(J^{PC}) = 0^+(1^{++})$.

REFERENCES

[1] R. Armenteros et al., Int. Conf. on Elementary Particle Physics, Siena, Italy, 1963.

[2] P. Baillon et al., Nuovo Cimento 50A (1967) 393.

[3] K.D. Duch et al., Z. Phys. C45 (1989) 223.

[4] C. Dionisi et al., Nucl. Phys. B169 (1980) 1.

[5] M.G. Rath et al.,Phys. Rev. D40 (1989) 693;

S.U. Chung et al., Phys. Rev. Lett. 55 (1985) 779;

A. Birman et al., Phys. Rev. Lett. 61 (1988) 1557.

[6] A. Ando et al., Phys. Rev. Lett. 57 (1986) 1296.

[7] T. Armstrong et al., Phys. Lett. B146 (1984) 273.

T. Armstrong et al., Z. Phys. C34 (1987) 23.

T. Armstrong et al., Phys. Lett. B221 (1989) 221.

[8] H. Aihara et al., Phys. Rev. Lett. 57 (1986) 2500;

G. Gidal et al., Phys. Rev. Lett. 59 (1987) 2016;

[9] Z. Bai et al., Phys. Rev. Lett. 65 (1990) 2507.

[10] J.J. Becker et al., Phys. Rev. 65 (1990) 2507.

[11] A.Palano, Proc. of the Hadronic Session of the XXII Rencontre de Moriond (1987), Ed. Frontiéres;

S.U. Chung, Z. Phys. C46, (1990) S111;

L. Köpke and N. Wermes, Phys. Rep. 174 (1989) 67.

[12] Ph. Gavillet et al., Z. Phys. C16 (1982) 119;

D. Aston et al., Phys. Lett. B201 (1988) 573.

[14] D.O. Caldwell, Mod. Phys. Lett. A2 (1987) 771;

[15] S. Ishida et al., Progress of Theoretical Phys. 82 (1989) 119.

[16] R.S. Longacre, Phys. Rev. D42 (1990) 874.

[17] J. Iizuka et al., Phys. Rev. D36 (1987) 1422;

J. Iizuka et al., Prog. Theor. Phys. 79 (1988) 141;

J. Iizuka et al., Phys. Rev. D39 (1989) 3357;

J. Iizuka et al., Prog. Theor. Phys. 86 (1991) 885.

[18] T. Armstrong et al., Nucl. Instr. and Meth. A276 (1989) 165.

[19] R. Ehrlich et al., Phys. Rev. Lett. 20 (1968) 686.

[20] S.I. Bityukov et al., Phys. Lett. B188 (1987) 383.

[21] T.A. Armstrong et al., Phys. Lett. B228 (1989) 536.

[22] T. Armstrong et al., Z. Phys. C52 (1991) 389.

[23] T. Armstrong et al., CERN-PPE/91-219, 29 Nov. 1991, submitted to Z.Phys. C.

[24] Ch. Zemach, Phys. Rev. B133 (1964) 1201.

FIGURE CAPTIONS

Fig. 1 (a) Ehrlich mass distribution for the reaction $(\pi^+/p)p \to (\pi^+/p)(K^0_S K^\pm \pi^\mp)p$ at 85 GeV/c and 300 GeV/c.

(b) $K^0_S K^\pm \pi^\mp$ effective mass distribution summed over all the data.

Fig. 2 (a) $\gamma\gamma$ effective mass distribution for events candidate to the $K^+K^-\pi^0$ final state;

(b) Ehrlich mass distribution for the events shown in (a).

(c) $K^+K^-\pi^0$ effective mass distribution;

(d) K^+K^- effective mass distribution in the $K^+K^-\pi^0$ final state.

Fig. 3 (a) $K^0_S K^0_S \pi^0$ effective mass for fully reconstructed events;

(b) $\pi^+\pi^-$ mass distribution in the V^0 for fully reconstructed events;

(c) $K^0_S K^0_S \pi^0$ effective mass for events having one missing γ;

(d) $\pi^+\pi^-$ mass distribution in the V^0 for events having one missing γ;

(e) $K^0_S K^0_S \pi^0$ effective mass obtained summing the histograms (a) and (c). The shaded histogram shows the $K^*\bar{K}$ contribution.

Fig. 4 Summary of the most important results obtained in this experiment on the $f_1(1285)$ and $E/f_1(1420)$ mesons.

(a) $K^0_S K^\pm \pi^\mp$ mass distribution summed over the 85 GeV/c and 300 GeV/c data,

(b) $2\pi^+2\pi^-$ effective mass from the 300 GeV/c data;

(c) $\eta\pi^+\pi^-$ effective mass from the 300 GeV/c data;

(d) $\rho^0\gamma$ effective mass from the 300 GeV/c data.

Fig. 5 Results from the Dalitz plot analysis of the $K^0_S K^\pm \pi^\mp$ system. The curves are the results from the fits described in the text.

Fig. 6 Expectations for different spin parity assignments for the distributions of the angles θ_1 and θ_2 described in the text. Full line: 0^{-+}, dashed line: 1^{++}, dotted line: 1^{+-}. The distributions have been generated assuming 50% of signal and 50% of phase space in the $K^*\bar{K}$ decay mode.

Fig. 7 Dalitz plot for the $E/f_1(1420)$ region ($1.37 < m(K\bar{K}\pi) < 1.49$ GeV).

Fig. 8 The Monte-Carlo simulation performed for hypothesis A : ($J^{PC} = 0^{-+}, 1^{++}, 1^{+-}$, phase space) is superimposed on the data.

Fig. 9 The Monte-Carlo simulation performed for hypothesis B : ($J^{PC} = 0^{-+}, 1^{+-}$, phase space) is superimposed on the data.

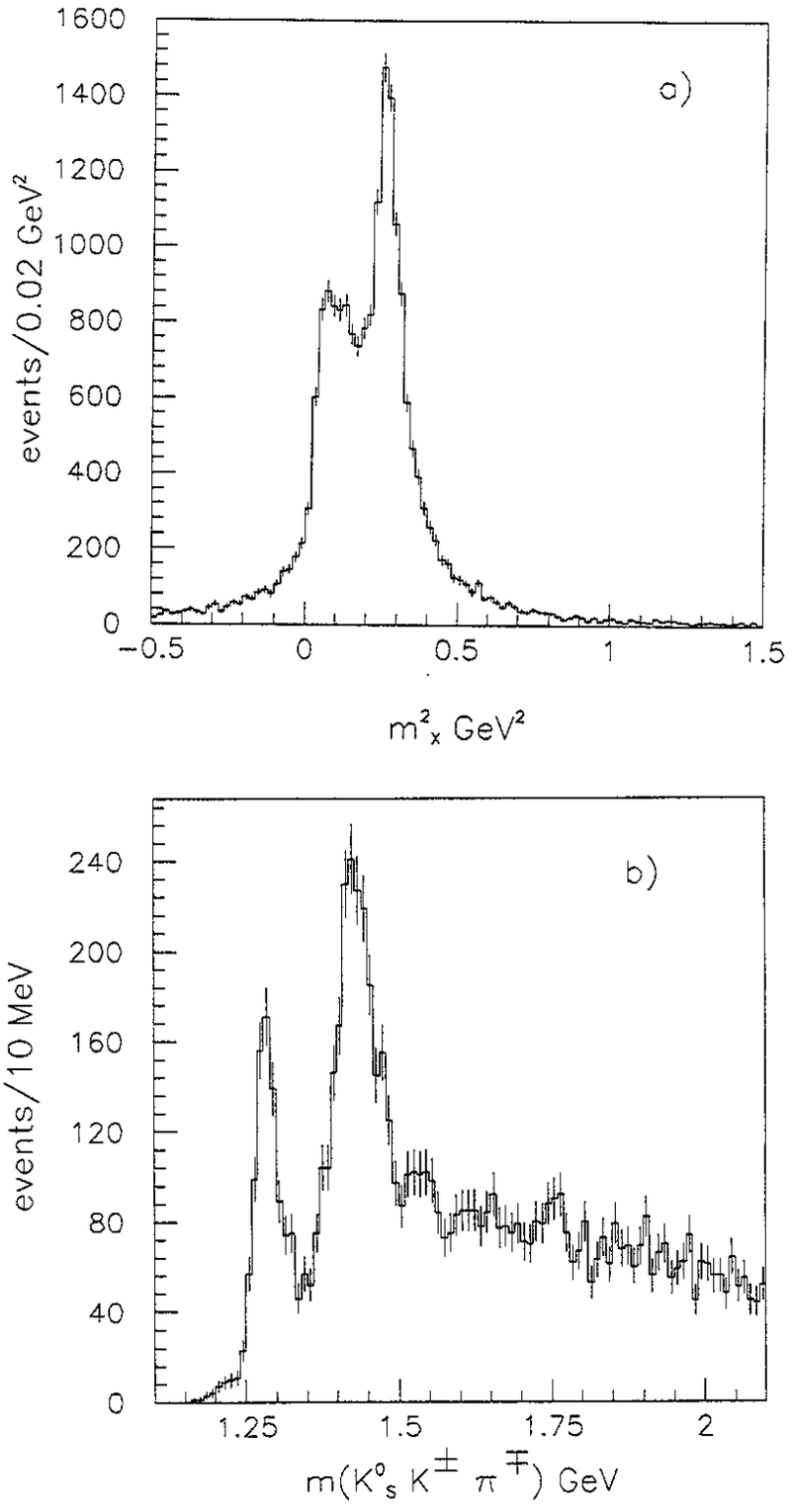
a)
events/0.02 GeV²
1600
1400
1200
1000
800
600
400
200
0
−0.5
0
0.5
1
1.5
m²x GeV²
b)
events/10 MeV
240
200
160
120
80
40
0
1.25
1.5
1.75
2
m(K°s K± π∓) GeV

Fig. 1

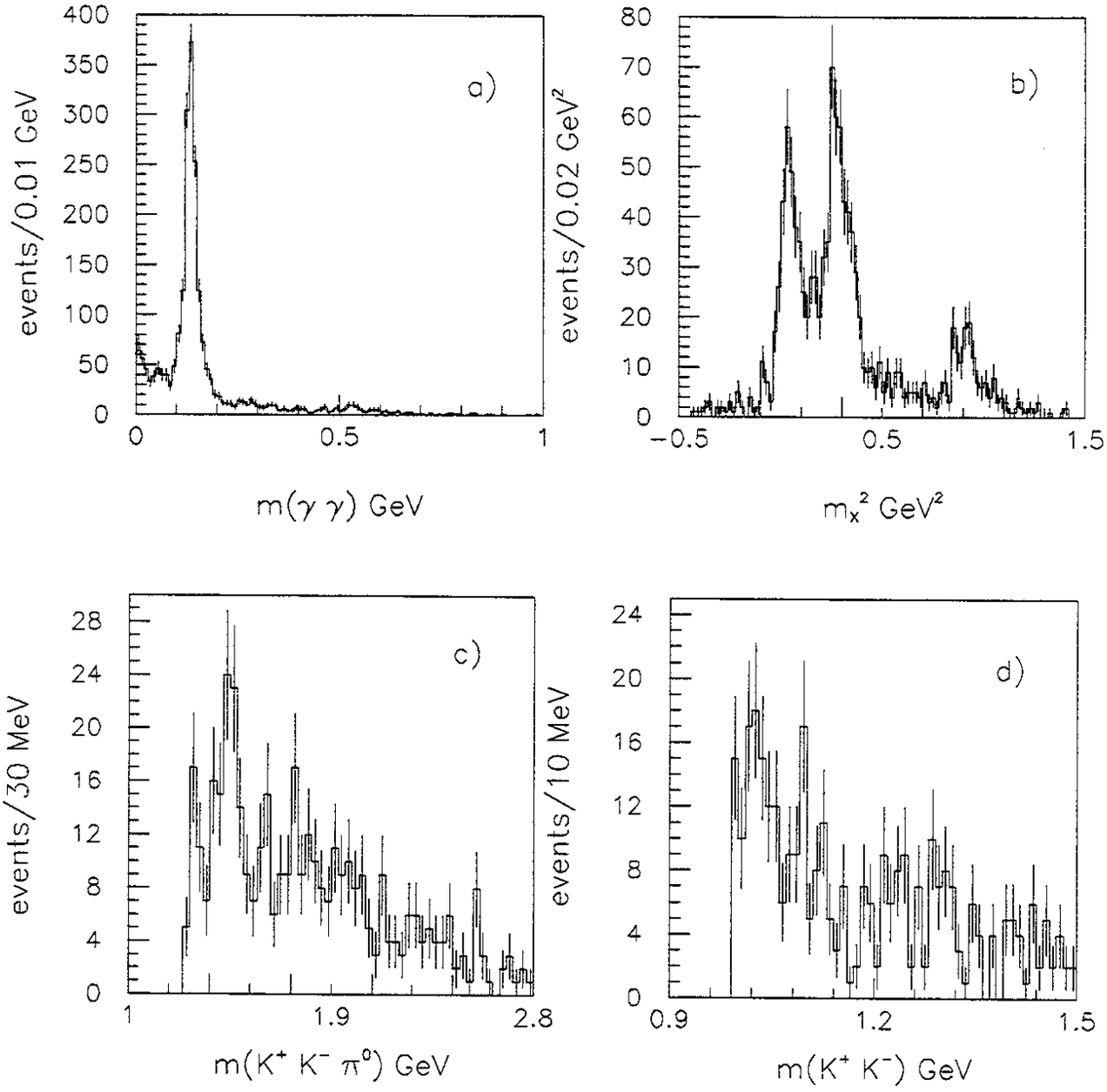
a)
b)
c)
d)
events/0.01 GeV
events/0.02 GeV²
events/30 MeV
events/10 MeV
m(γ γ) GeV
m_x² GeV²
m(K⁺ K⁻ π⁰) GeV
m(K⁺ K⁻) GeV

Fig. 2

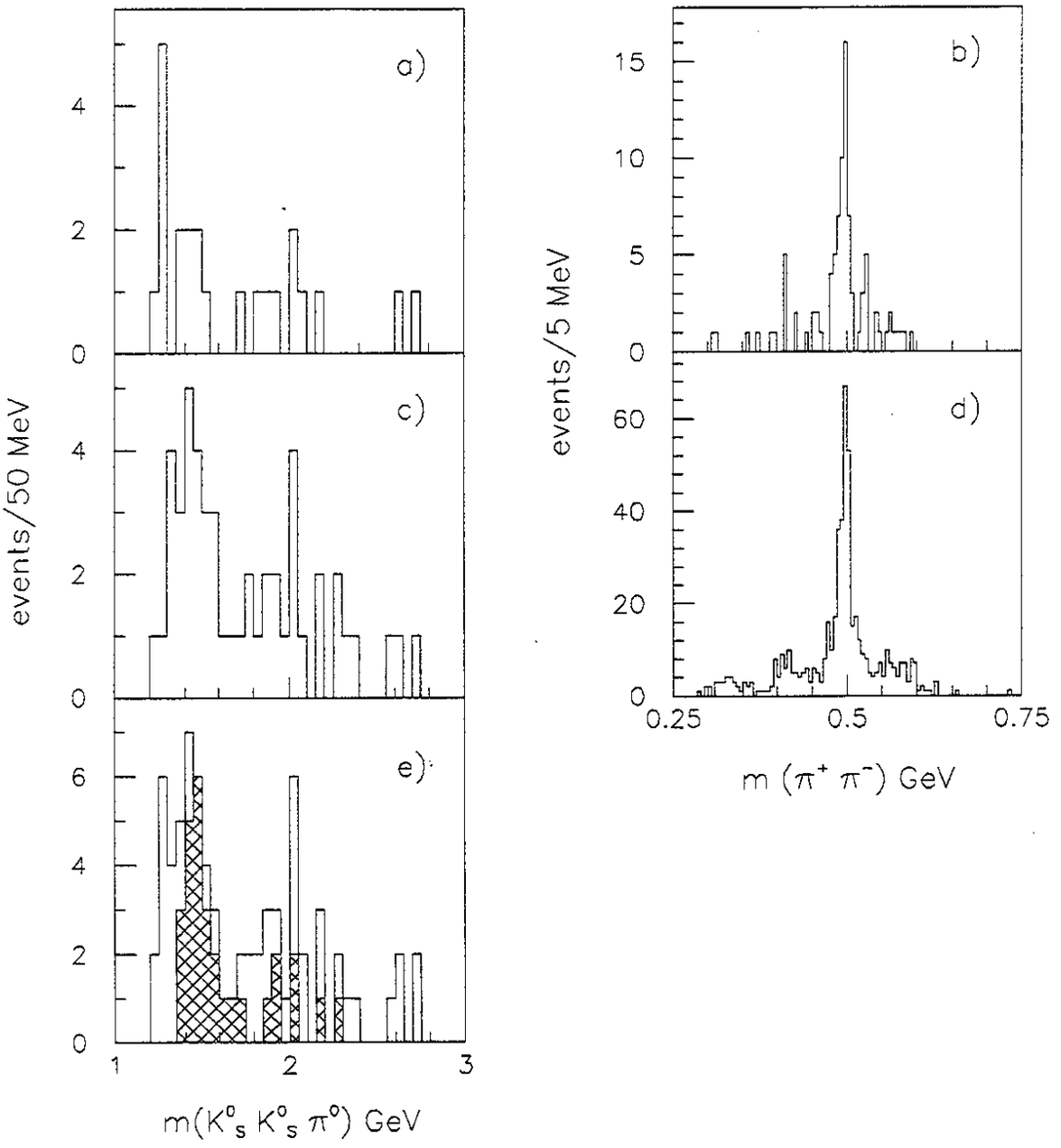

Fig. 3

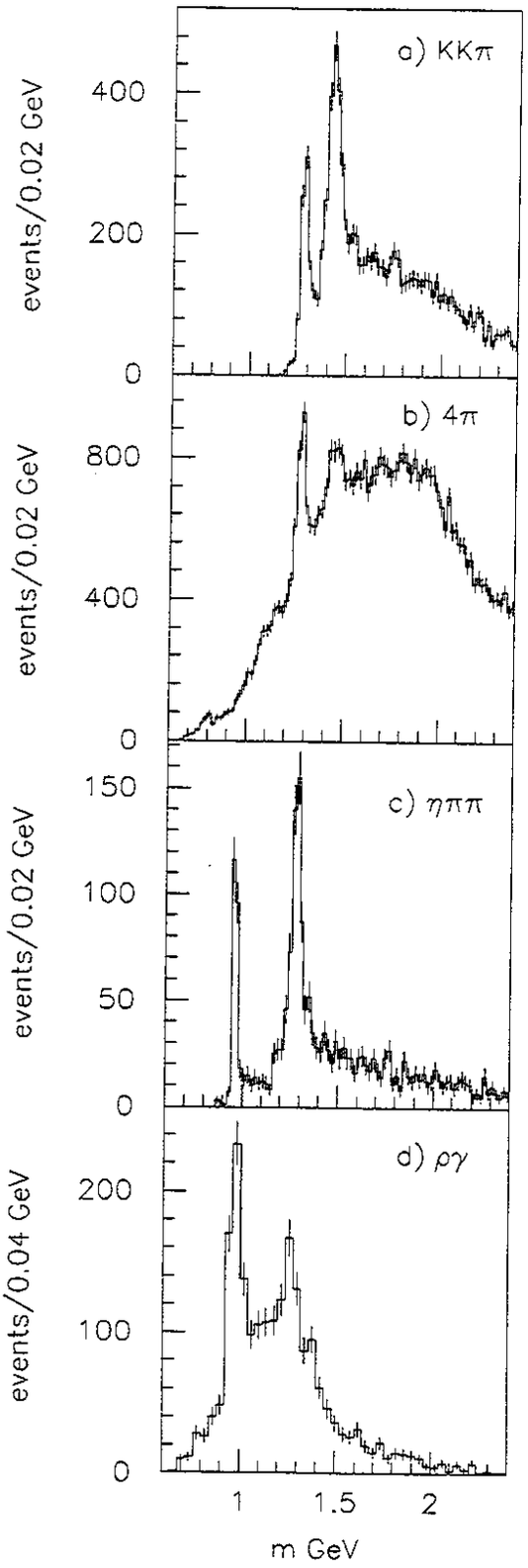
a) KKπ
b) 4π
c) ηππ
d) ργ
events/0.02 GeV
events/0.02 GeV
events/0.02 GeV
events/0.04 GeV
400
200
0
800
400
0
150
100
50
0
200
100
0
1
1.5
2
m GeV

Fig. 4

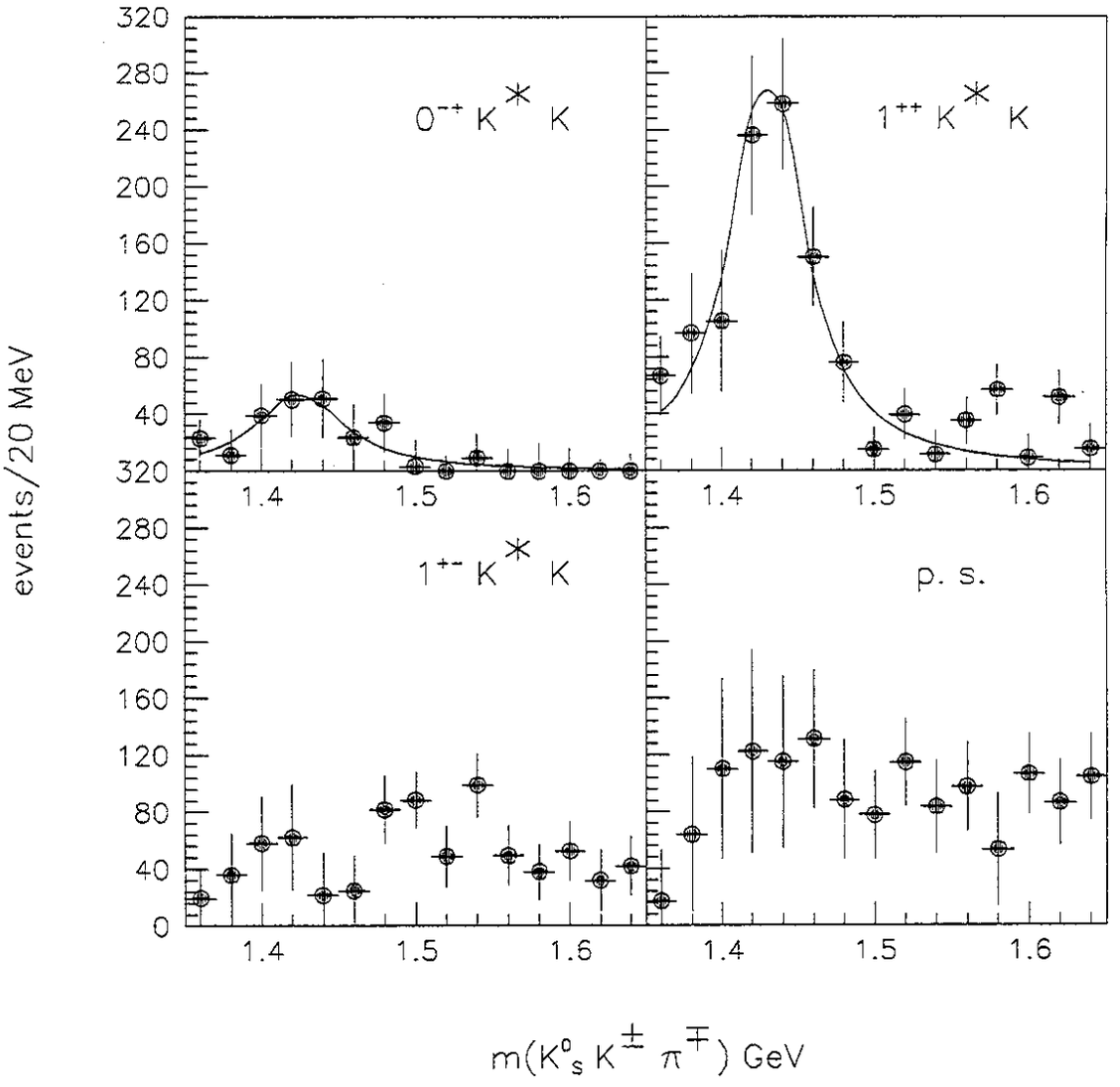

Fig. 5

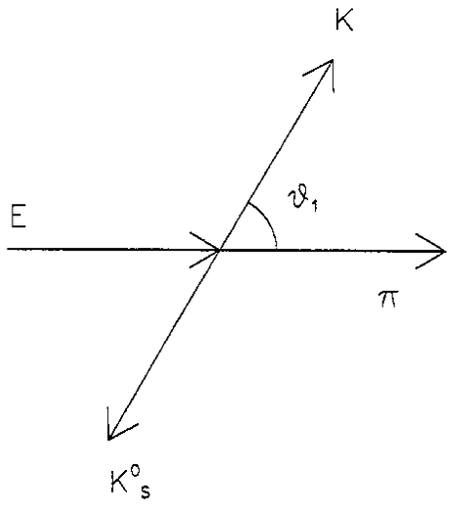
K
E
ϑ_1
π
K^o_s

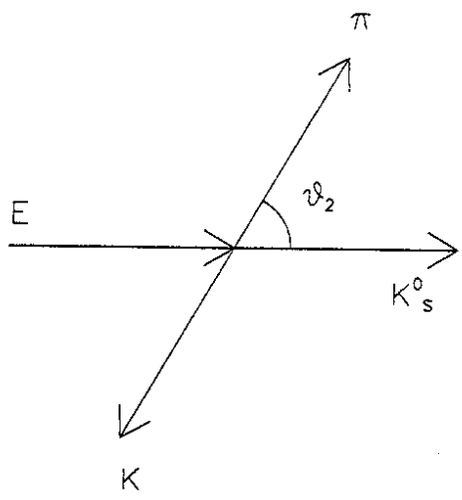
π
E
ϑ_2
K^o_s
K

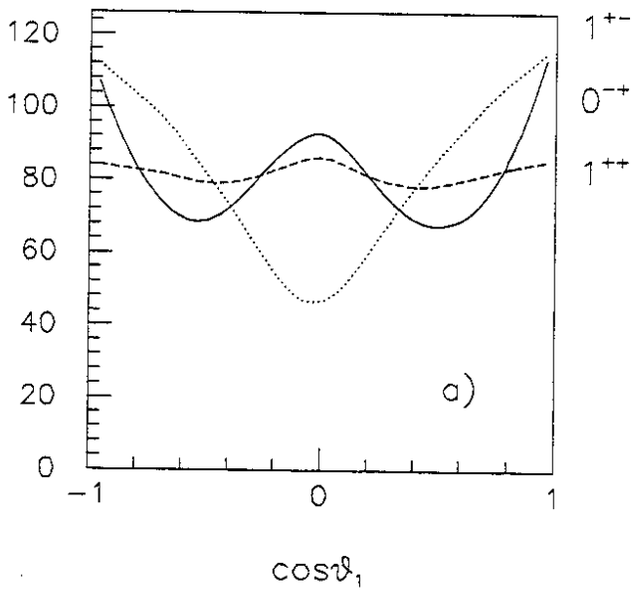
120
100
80
60
40
20
0
−1
0
1
1^{+-}
0^{-+}
1^{++}
a)
$\cos\vartheta_1$

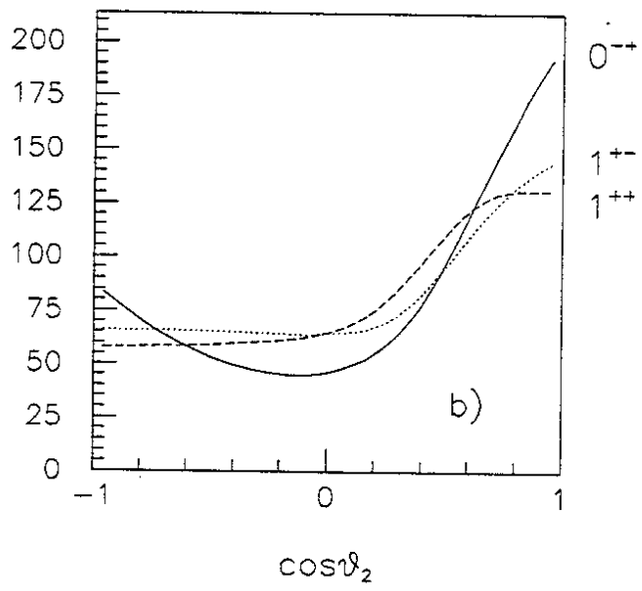
200
175
150
125
100
75
50
25
0
−1
0
1
0^{-+}
1^{+-}
1^{++}
b)
$\cos\vartheta_2$

Fig. 6

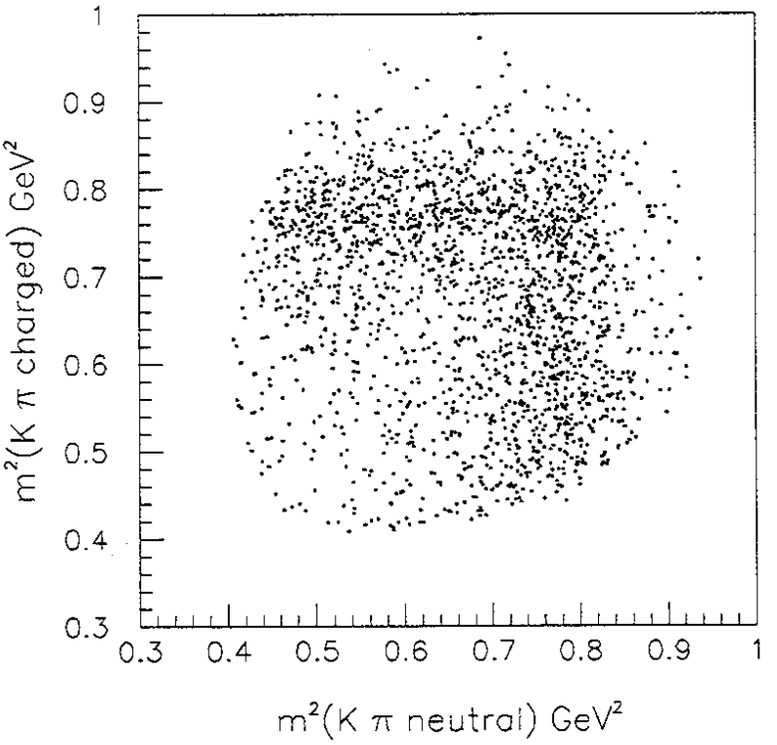
1
0.9
0.8
0.7
0.6
0.5
0.4
0.3
0.3
0.4
0.5
0.6
0.7
0.8
0.9
1
m²(K π charged) GeV²
m²(K π neutral) GeV²

Fig. 7

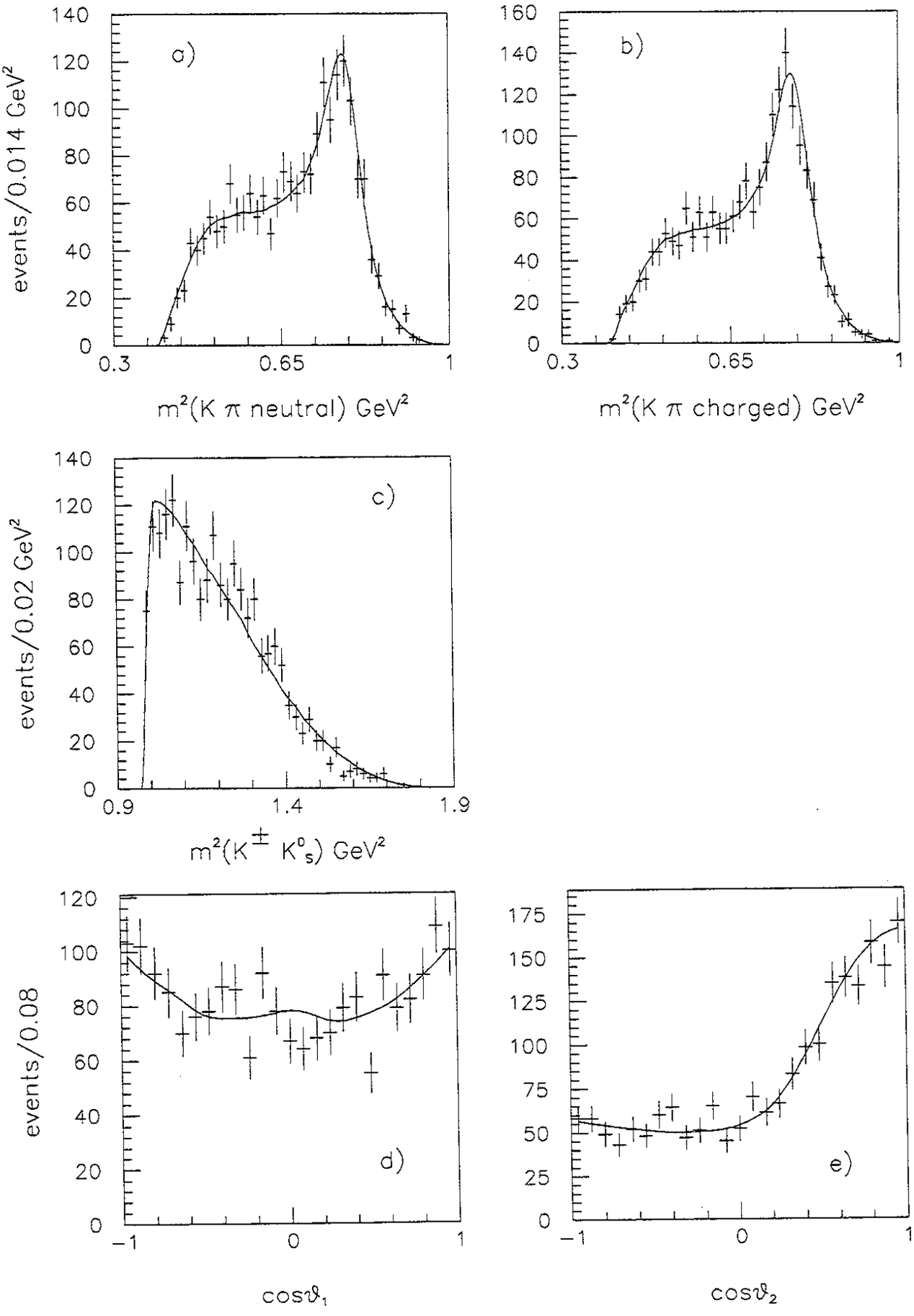
a)
b)
c)
d)
e)
events/0.014 GeV²
m²(K π neutral) GeV²
m²(K π charged) GeV²
events/0.02 GeV²
m²(K± K⁰s) GeV²
events/0.08
cosϑ₁
cosϑ₂

Fig. 8

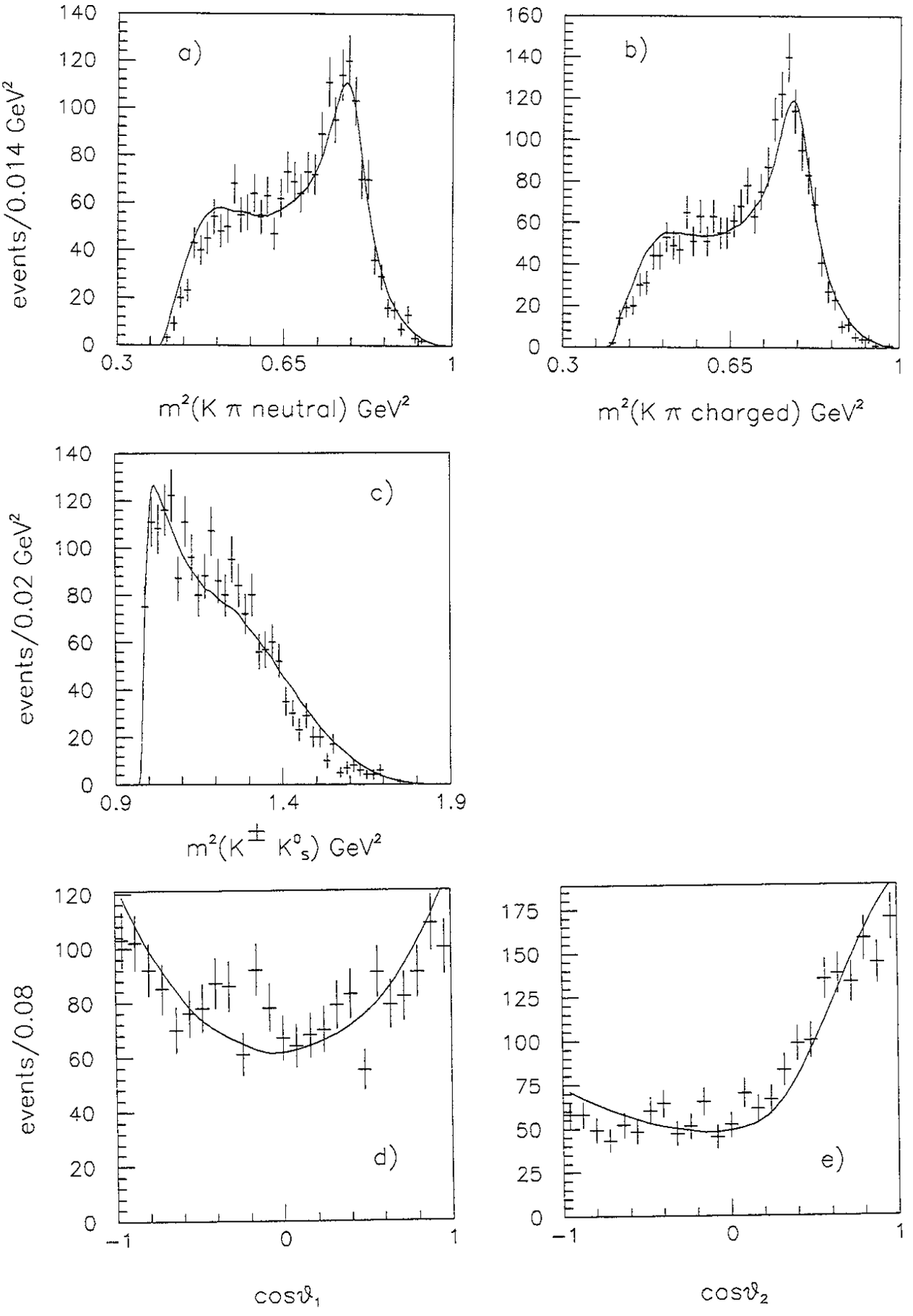
a)
b)
c)
d)
e)
events/0.014 GeV²
m²(K π neutral) GeV²
m²(K π charged) GeV²
events/0.02 GeV²
m²(K± K⁰s) GeV²
events/0.08
cosϑ₁
cosϑ₂

Fig. 9